ISSN 0967-0912, Steel in Translation, 2019, Vol. 49, No. 6, pp. 377–383. © Allerton Press, Inc., 2019.
Russian Text © The Author(s), 2019, published in Izvestiya Vysshikh Uchebnykh Zavedenii, Chernaya Metallurgiya, 2019, No. 6, pp. 438–445.

Influence of the Surface Structure and Properties on the Fatigue Strength of Electromechanically Strengthened Quenched Steel

V. P. Bagmutov[a], *, N. G. Dudkina[a], I. N. Zakharov[a], M. D. Romanenko[a], and V. V. Chekunov[a]

[a] *Volgograd State Technical University, Volgograd, 400005 Russia*

**e-mail: sopromat@vstu.ru*

Received February 11, 2018; revised March 11, 2018; accepted March 21, 2018

Abstract—For the example of quenched carbon steel 45 and U8 steel, the influence of surface hardening (electromechanical treatment, surface plastic deformation, nonabrasive ultrasonic finishing, and various combinations) on the surface structure and microhardness, the cyclic durability of the hardened samples, and the mechanisms of fatigue failure is analyzed. Research by means of optical and scanning electron microscopy, microhardness measurement, and fatigue tests shows that, for the quenched carbon steels, high-speed pulsed thermal deformation in the course of electromechanical treatment increases the surface microhardness (by more than 50%) and decreases the fatigue limit (by 20–30%). That is associated with the formation of hard nonequilibrium ultradisperse phases of nonuniform chemical composition in the surface layer. The quenched structure close to the surface is tempered, with the formation of softening zones and the appearance of residual tensile stress. Accordingly, the microhardness in these zones declines and the fatigue limit falls. Such decrease in performance of the steel on surface hardening merits further study, along with potential technologies for improving its performance. Surface hardening of carbon steels by some combination of electromechanical treatment, surface plastic deformation, and nonabrasive ultrasonic finishing permits adjustment of the structure and phase composition and the stress–strain state of surface and subsurface layers of the steel by varying the temperature and deformation. By that means, balanced strength and fatigue characteristics of the samples may potentially be obtained by appropriate preliminary heat treatment. Intense surface plastic deformation and nonabrasive ultrasonic finishing after electromechanical hardening may be used to smooth the surface, mend subsurface defects, and correct the stress–strain state of the steel. That increases the microhardness in the tempering zone by 20–25% and the fatigue limit of the samples by 25–30%.

Keywords: electromechanical treatment, surface plastic deformation, nonabrasive ultrasonic finishing, microhardness, fatigue strength, microstructure

DOI: 10.3103/S0967091219060020

INTRODUCTION

The performance of structural metal alloys may be improved by creating ultradisperse structures in the surface layer with the distinctive physicomechanical properties required in rigorous operating conditions. Combinations of thermal and mechanical treatments are often used to obtain the required properties: for example, various combinations [12, 13] of chemicothermal methods [1, 2]; laser treatment [2, 3], plasma treatment [4], shock treatment [5, 6], ultrasound treatment [3, 7], electron-beam treatment [8, 9], and electroexplosive alloying [10, 11].

Combinations of surface-hardening electromechanical treatment [14] with surface plastic deformation [15, 16], shock treatment [17], frictional hardening [18, 19], diamond smoothing [20], ultrasound treatment [21], and plasma spraying [22–24] are used for a wide range of structural materials, such as steels [15–21], titanium and aluminum alloys [25–27], and coatings [22–24].

Attention focuses on the structure [15, 17, 19, 25, 26], depth, hardness, and other properties of the hardened layer [15–18, 21, 23–25] and the operational characteristics (wear resistance [18, 22] and fatigue strength [15, 26]) of the hardened samples.

Note that the creation of a layer of elevated hardness on the sample surface may be accompanied by embrittlement; the formation of unfavorable residual stress; greater likelihood of cracking; and hence decrease in fatigue strength and in resistance to nonabrasive, cavitational, and erosional wear. Such behavior is noted in titanium alloys, plasma coatings, and quenched steels, for example. Little is known about the mechanisms by which the operational characteristics of such materials decline on surface harden-

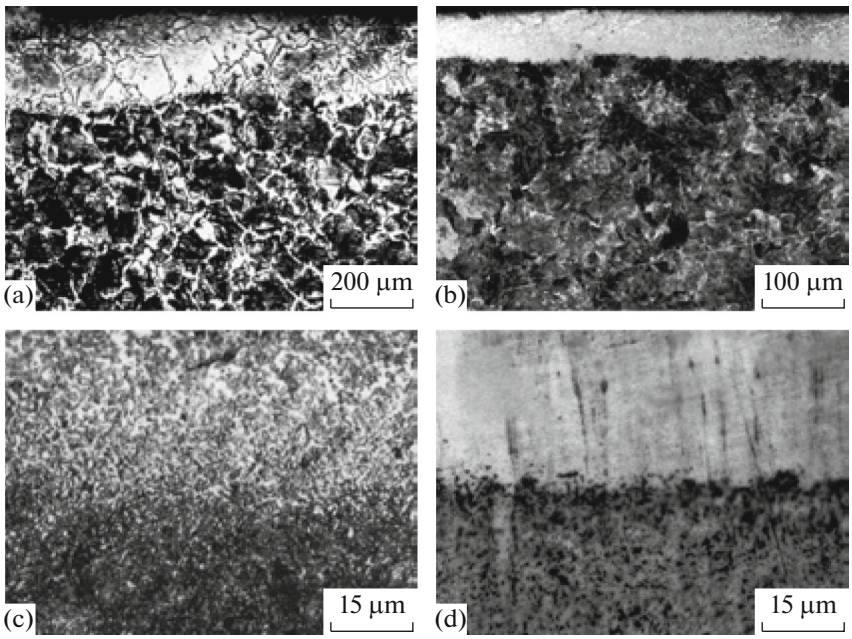

Fig. 1. Microstructure of normalized steel 45 (a) and U8 steel (b) and quenched steel 45 (c) and U8 steel (d) after electromechanical treatment.

ing. Consequently, few corrective measures have been identified.

In this context, we need to develop surface hardening technologies that produce balanced performance of the treated product (in terms of hardness, wear resistance, strength, and durability).

In the present work, we investigate the change in fatigue strength of quenched carbon steels under the action of various combinations of surface-hardening technologies: electromechanical treatment, surface plastic deformation, and nonabrasive ultrasonic finishing [28].

EXPERIMENTAL MATERIALS AND METHODS

We compare the properties of moderate-carbon structural steel 45 and U8 carbon tool steel after quenching and low tempering.

Cylindrical samples of the steel are produced in accordance with State Standard GOST 22502–79 (type 1) and subjected to surface hardening by various methods: electromechanical treatment, electromechanical treatment + surface plastic deformation, and electromechanical treatment + nonabrasive ultrasonic finishing. The diameter of the samples' working section is 7.5 mm.

In electromechanical treatment, an alternating current (density $j = 400$ A/mm^2) is applied at voltage $U = 4$–5 V through the local contact zone of the tool (a hard-alloy roller) to the sample surface. The rate of treatment $V = 0.31$ m/min; the supply $S = 0.4$–0.8 mm/turn; and the force on the tool $F = 200$–1000 N.

In surface plastic deformation, a roller is applied with force $F = 400$–1200 N. The rate of treatment $V = 0.31$ m/min; the supply $S = 0.25$ mm/turn; and the number of turns $n = 1$. The roller diameter is 36 mm, and the rounding radius is 4 mm.

In nonabrasive ultrasonic finishing, the conditions are as follows: vibrational frequency of tool 22 kHz; rate of treatment $V = 4.71$ m/min; the tool supply is 0.07 mm/turn; and the force on the hard-alloy tool $F = 100$ N.

The microhardness is measured by means of a PMT-3M instrument; the indenter load is 50 g. The microstructure is studied by means of a METAM LV-32 microscope and a Versa 3D scanning electron microscope.

We use an NU-3000 fatigue-testing machine for cyclic loading by pure flexure with rotation. The loading frequency is 50 Hz; the loading cycle is symmetric; and the baseline number of cycles is $N = 20 \times 10^6$.

STEEL STRUCTURE AFTER ELECTROMECHANICAL TREATMENT

In Fig. 1, we show the microstructure of the surface layers of 45 and U8 steel samples hardened by electromechanical treatment after preliminary normalization (Figs. 1a and 1b) and quenching (Figs. 1c and 1d).

At the surface of all the samples after electromechanical treatment, we observe a characteristic white layer, consisting of hard ultradisperse martensitic

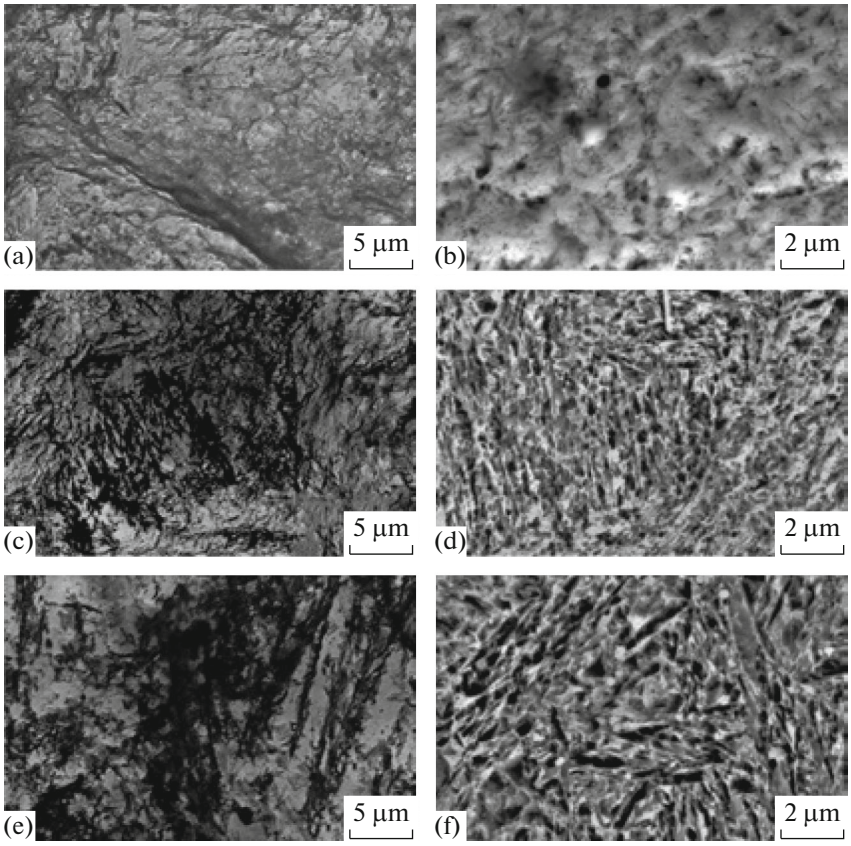

Fig. 2. Microstructure in different regions over the surfaced layer of quenched steel 45 (a, c, e) and U8 steel (b, d, f) after electromechanical treatment: (a, b) hardening zone; (c, d) tempering zone; (e, f) initial structure.

structure. The white layer does not contain acicular or other characteristic crystalline structure and appears as a continuous bright field (Fig. 1).

The hardened layer on the surface of normalized steel (Figs. 1a and 1b) differs from that of quenched samples (Figs. 1c and 1d) in that its structure is less uniform. With relatively coarse initial structure of the metal (with ferrite–pearlite or pearlite structure), the ultradisperse martensite formed at the pearlite may inherit the internal texture, retaining the pattern of cementite and ferrite sections, as well as the ferrite grid along the grain boundaries (Figs. 1a and 1b). For steel 45 (Fig. 1a) with initial ferrite–pearlite structure, the nonuniformity of the surface layer is more pronounced than for U8 steel with pearlite structure (Fig. 1b).

For the steel that initially undergoes quenching and low tempering, the initial structure (tempering martensite) is more uniform. That is reflected in the structure of the hardened surface (Figs. 1c and 1d). With increase in carbon content in the steel, the white layer becomes more uniform (Fig. 1).

At a certain depth, a zone of increased etchability is seen in the white layer on the quenched steels. It takes the form of a dark frame around the hardened fragment (Figs. 1c and 1d). This zone corresponds to weakening (tempering) of the material. The size of this region in the initial steel depends on its preliminary heat treatment. After quenching and low tempering, the zone of increased etchability is of maximum size: 0.25–0.35 mm.

Electron microscopic analysis of the quenched steels indicates that, after electromechanical treatment, the microstructure of the metal in the characteristic zones of the surface layer is very different (Fig. 2).

In the hardened layer, we note structure typical of rapid quenching at high magnification (12000–30000×): structureless martensite (nonacicular martensite with latent crystalline structure), with small inclusions of carbides and residual austenite (Figs. 2a and 2b).

In the zone of increased etchability at a depth of 150–500 μm below the hardened white layer, we observe different structures formed by martensite decomposition (Figs. 2c and 2d). Their distribution over the volume of this zone depends on the temperature and its gradients over space and time. For exam-

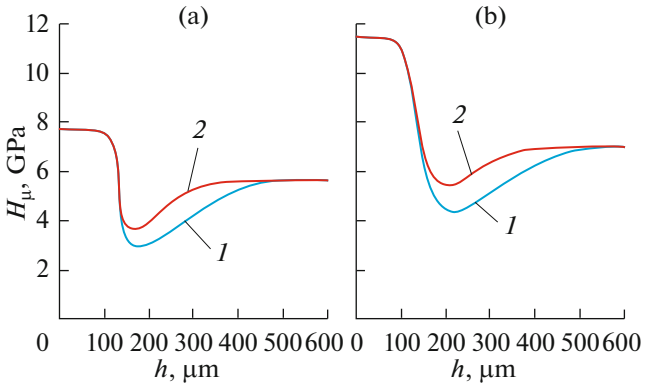

Fig. 3. Microhardness H_μ as a function of the depth h of the surface layer in quenched steel 45 (a) and U8 steel (b) after electromechanical treatment (*1*) and electromechanical treatment + surface plastic deformation (*2*).

ple, adjacent to the boundary of the hardened layer, where the temperatures are significant in electromechanical treatment but the cooling rate is insufficient for quenching, we observe high-temperature tempering of the initial martensitic structure, with the formation of sorbite. On moving away from the hardened layer, the temperature in the thermal-influence zone falls. At some depth (around 300–400 μm), besides sorbite, we note regions with tempering-troostite structure. With decrease in temperature over the depth of the tempering zone, the content of troostite regions increases.

At a depth of around 500–600 μm, we observe volumes of metal with a low content of tempered martensite. At the boundary of the tempering zone with the initial structure, we mainly see tempering martensite with a smooth transition to the structure of the initial material. Beyond 500–600 μm, we observe the initial structure of the quenched steel, with typical small and medium-sized martensite needles (Figs. 2e and 2f).

MICROHARDNESS AFTER ELECTROMECHANICAL TREATMENT AND SURFACE PLASTIC DEFORMATION

In Fig. 3, we show measurements of the surface microhardness of quenched steel 45 (Fig. 3a) and U8 steel (Fig. 3b) after electromechanical treatment (*1*) and electromechanical treatment + surface plastic deformation (*2*).

The white layer (depth around 120–180 μm) is characterized by elevated mean microhardness: 7.5–8.0 GPA for steel 45 and 8.5–9.0 GPa for U8 steel. In other words, the microhardness is 1.5 times that in the initial state (after quenching and low tempering). With increase in carbon content in the steel, the microhardness and depth of the hardened layer increase (Fig. 3), on account of the increased dispersity of the initial steel structure and the deposition of carbide phase [29].

The boundary of the hardened and softened metal for quenched steel is characterized by sharp decline from the hardness of the white layer (7.5–9.0 GPa) to the hardness of the thermal-influence zone (3.5–4.5 GPa), as we see in Fig. 3. The depth of the thermal-influence zone is around 300–350 μm. The drop in microhardness in this region is due to the formation of martensite decomposition products on tempering. The smooth microhardness variation in the thermal-influence zone (to the initial value of 6.0–6.5 GPa) is associated with gradual transition in structure on approaching the quenched core (Fig. 3).

After electromechanical treatment, additional surface plastic deformation has practically no influence on the microhardness of the white layer but increases the hardness in the secondary-tempering zone (Fig. 3, curve *2*). The microhardness increases on account of hardening (cold working) of the tempered metal. Metals with lower initial hardness undergo greater hardening. The minimum microhardness in the secondary-tempering zone is increased by 25–30% (around 1 GPa) after electromechanical treatment + surface plastic deformation and gradually increases to the hardness of the quenched core. The width of the softened zone decreases simultaneously by 100–150 μm (Fig. 3, curve *2*).

FATIGUE STRENGTH OF STEEL AFTER ELECTROMECHANICAL TREATMENT

We know that the presence of high-strength white-layer segments at the surface of normalized steel samples markedly increases the fatigue strength [15]. For example, for normalized steel 45, the fatigue limit increases from 370 to 450 MPa (by more than 20%) after electromechanical treatment, while the fatigue life increases more than fivefold [15].

For steel subjected to quenching and low tempering (steel 45 and U8 steel in the present work), the fatigue characteristics in cyclic loading may decrease after electromechanical treatment (Fig. 4, curve *2*). The fatigue limit of quenched steel 45 (Fig. 4a) falls from 650 to 530 MPa after electromechanical treatment (by 20%), while that of quenched U8 steel (Fig. 4b) falls from 930 to 650 MPa (by 30%).

Additional plastic deformation (surface plastic deformation or nonabrasive ultrasonic finishing) after electromechanical treatment increases the fatigue characteristics of the steel.

As we see in Fig. 4a, the fatigue limit of quenched steel 45 after electromechanical treatment + surface plastic deformation is increased by 35% (from 520 to 690 MPa) in comparison with the sample after electromechanical treatment (curves *2* and *3*) and by 7%

(from 650 MPa) in comparison with the initial (quenched) samples (curve *1*). The initial fatigue life of the samples is increased sixfold by electromechanical treatment + surface plastic deformation (Fig. 4a).

For quenched U8 steel, additional nonabrasive ultrasonic finishing increases the fatigue limit of the sample after electromechanical treatment by 26% (from 650 to 822 MPa), while additional surface plastic deformation increases the fatigue limit by 31% (from 650 to 856 MPa). However, the corresponding fatigue strength is still lower than that for the initial quenched samples (930 MPa).

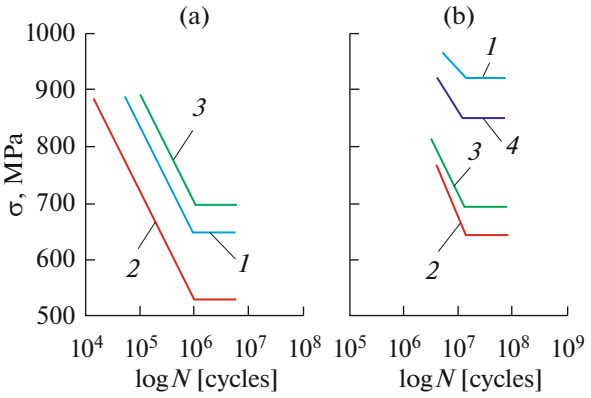

Fig. 4. Fatigue curves of steel 45 (a) and U8 steel (b) after quenching and tempering at 300°C (*1*), after electromechanical treatment (*2*), after electromechanical treatment + surface plastic deformation (*3*), and after electromechanical treatment + nonabrasive ultrasonic finishing (*4*).

DISCUSSION OF THE RESULTS

Surface hardening of steel by electromechanical treatment is characterized by high rates of heating (10^5–10^6°C/s) and cooling (10^4–10^5°C/s) [30], with simultaneous plastic deformation. Such treatment may produce structure with specific properties that are not easily attainable in standard heat treatment or thermomechanical treatment.

In the surface layer of the steels after electromechanical treatment, we find a hardened ultrafine-grain martensite structure, characterized by little dilation of the fragments, quasi-uniform mechanical properties, and high corrosion resistance. Metallographic data show this structure in the form of a practically continuous hard white layer.

As well as high-speed quenching at the surface of the steel, the brief high temperatures created during electromechanical treatment lead to rapid tempering of the initial structure (in the case of quenched steel) and self-tempering of the newly hardened structure. As a result, the surface layer of quenched steels after electromechanical treatment may contain a broad range of structural states with hardness less than in the hardened layer. In this softening zone, the microhardness varies from a minimum value (adjacent to the hardened layer, where the tempering temperature is greatest) to the initial hardness of the quenched metal (as the temperature declines over the depth).

The formation of high-strength white-layer structure at the sample surface retards the nucleation and development of fatigue cracks and decreases the content of discontinuities and microscopic stress concentrators in the surface layer. For normalized steels, that increases the cyclic strength.

The appearance of the softened zone after the electromechanical treatment of quenched steels switches the influence of surface treatment on the fatigue strength of the samples [15]. The decomposition of the martensite structure in the given zone is accompanied by decrease in strength of the metal. In addition, the structural changes in that zone create residual tensile stress, according to modeling data [30]. Consequently, in fatigue tests with cyclic flexure and rotation, when the softened layer is close to the region of maximum active stress, we note intense accumulation of fatigue damage in the thermal-influence zone and the onset of fatigue failure.

The influence of surface deformation on the fatigue limit of steels after quenching and electromechanical treatment is associated primarily with mechanical strengthening of the metal in the surface layers, with consequent slowing of fatigue-defect development. In surface plastic deformation and nonabrasive ultrasonic finishing of steel samples after quenching and electromechanical treatment, the strain rate is greatest in the vicinity of the hardened segment and in the surrounding thermal-influence zone [30]. That switches the residual stress in this region from tensile to compressive, thereby further obstructing the formation and growth of fatigue cracks and improving sample life.

CONCLUSIONS

For the example of quenched carbon steel 45 and U8 steel, high-speed pulsed thermal and deformational treatment—specifically, electromechanical treatment—increases the surface microhardness (by more than 50%) and decreases the fatigue limit (by 20–30%). That is associated with tempering of the quenched structure close to the surface, with the formation of softening zones and the appearance of residual tensile stress.

Intense surface plastic deformation and nonabrasive ultrasonic finishing after electromechanical hardening may be used to smooth the surface, mend subsurface defects, and correct the stress–strain state of the steel. That increases the microhardness in the tem-

pering zone by 20–25% and the fatigue limit of the samples by 25–30%.

Surface hardening of carbon steels by some combination of electromechanical treatment, surface plastic deformation, and nonabrasive ultrasonic finishing permits adjustment of the structure and phase composition and the stress–strain state of surface and subsurface layers of the steel by varying the temperature and deformation. By that means, balanced strength and fatigue characteristics of steel samples may potentially be obtained by appropriate preliminary heat treatment.

FUNDING

Financial support was provided by the Russian Foundation for Basic Research (projects nos. 17-08-01742a and 18-48-340010 r_a).

REFERENCES

1. Garcia-Giron, A., Romano, J.M., Liang, Y., Dashtbozorg, B., et al., Combined surface hardening and laser patterning approach for functionalizing stainless steel surfaces, *Appl. Surf. Sci.*, 2018, vol. 439, pp. 516–524.
2. Lu, J., Huang, T., Liu, Zh., Zhang, X., and Xiao, R., Long-term wettability of titanium surfaces by combined femtosecond laser micro/nano structuring and chemical treatments, *Appl. Surf. Sci.*, 2018, vol. 459, pp. 257–262.
3. Lesyk, D.A., Martinez, S., Mordyuk, B.N., Dzhemelinskyi, V.V., et al., Effects of laser heat treatment combined with ultrasonic impact treatment on the surface topography and hardness of carbon steel AISI 1045, *Opt. Laser Technol.*, 2019, vol. 111, pp. 424–438.
4. Tsuji, N., Tanaka, S., and Takasugi, T., Effect of combined plasma-carburizing and deep-rolling on notch fatigue property of Ti–6Al–4V alloy, *Mater. Sci. Eng., A*, 2009, vol. 499, nos. 1–2, pp. 482–488.
5. Gill, A.S., Telang, A., Ye, C., et al., Localized plastic deformation and hardening in laser shock peened, *Mater. Charact.*, 2018, vol. 142, pp. 15–26.
6. Borko, K., Hadzima, B., and Jacková, M.N., Corrosion resistance of Domex 700 steel after combined surface treatment in chloride environment, *Procedia Eng.*, 2017, vol. 192, pp. 58–63.
7. Chenakin, S.P., Mordyuk, B.N., and Khripta, N.I., Surface characterization of a ZrTiNb alloy: Effect of ultrasonic impact treatment, *Appl. Surf. Sci.*, 2019, vol. 470, pp. 44–55.
8. Zenker, R., Electron meets nitrogen: combination of electron beam hardening and nitriding, *Int. Heat Treat. Surf. Eng.*, 2009, vol. 3, no. 4, pp. 141–146.
9. Ivanov, Yu.F., Gromov, V.E., Konovalov, S.V., Zagulyaev, D.V., Petrikova, E.A., and Semin, A.P., Modification of structure and surface properties of hypoeutectic silumin by intense pulse electron beams, *Prog. Phys. Met.*, 2018, vol. 19, no. 2, pp. 197–222.
10. Romanov, D.A., Sosnin, K.V., Gromov, V.E., Bataev, V.A., Ivanov, Yu.F., Glezer, A.M., and Sundeev, R.V., Titanium–zirconium coatings formed on the titanium implant surface by the electroexplosive method, *Mater. Lett.*, 2019, vol. 242, pp. 79–82.
11. Ivanov, Yu.F., Gromov, V.E., Soskova, N.A., Denisova, Yu.A, Teresov, A.D., Petrikova, E.A., and Budovskikh, E.A., Electron-beam surface treatment of alloys based on titanium, modified by plasma from an electrical explosion of conducting material, *Bull. Russ. Acad. Sci.: Phys.*, 2012, vol. 76, no. 11, pp. 1246–1252.
12. Bashchenko, L.P., Ivanov, Yu.F., and Budovskikh, E.A., Modification of the titanium VT1-0 surface layers structure after electroexplosive carboboronizing and electron-beam treatment, *Izv. Vyssh. Uchebn. Zaved., Chern. Metall.*, 2013, no. 3, pp. 68–70.
13. Ivanov, Yu.F., Budovskikh, E.A., Gromov, V.E., Bashchenko, L.P., Soskova, N.A., and Raikov, S.V., Formation of nanocomposite layers at the surface of VT1-0 titanium in electroexplosive carburization and electron-beam treatment, *Steel Transl.*, 2012, vol. 42, no. 6, pp. 499–501.
14. Edigarov, V.R., *Tekhnologii i oborudovanie kombinirovannykh sposobov elektromekhanicheskoi obrabotki* (Technologies and Equipment of Combined Methods of Electromechanical Processing), Omsk: Omsk. Tankovyi Inzh. Inst., 2014.
15. Dudkina, N.G., Evaluation of fatigue strength of heat-treated medium-carbon structural steel after combined hardening (EDM + + SPD), *Mechanika* (Lietuva), 1998, no. 4, pp. 28–32.
16. Edigarov, V.R. and Litau, E.V., Study of some technological aspects of the new combined method of EDMt + SPD surface treatment of hardened steels, *Nats. Prioritety Rossii. Ser. 1: Nauka Voen. Bezop.*, 2015, vol. 3, no. 3, pp. 125–130.
17. Matlin, M.M., Dudkina, N.G., and Dudkin, A.D., Features of formation of hardened layer under electromechanical processing with dynamic force impact, *Uprochnyayushchie Tekhnol. Pokrytiya*, 2007, no. 6, pp. 39–40.
18. Yakovlev, S.A., Wear resistance of machine parts after antifriction electromechanical processing, *Vestn. Ul'yanovsk. Gos. S-kh. Akad.*, 2011, no. 3, pp. 116–120.
19. Edigarov, V.R. and Kilunin, I.Yu., Radiographic study of 38KhS steel, subjected to frictional-electric modification, *Metalloobrabotka*, 2011, no. 4, pp. 24–29.
20. Yakovleva, A.P. and Omel'chenko, I.S., Increase of load capacity of steel parts by combined processing, *Aviats. Prom-st'.*, 2013, no. 2, pp. 62–64.
21. Edigarov, V.R., Alimbaeva, B.Sh., and Perkov, P.S., Combined electromechanical ultrasonic treatment of surface layers of machine parts, *Vestn. Sib. Gos. Avtom.-Dorozhn. Akad.*, 2017, vol. 54, no. 2, pp. 42–47.
22. Ivannikov, A.Yu., Kalita, V.I., Komlev, D.I., et al., The effect of electromechanical treatment on structure and properties of plasma sprayed Fe–6W–5Mo–4Cr–2V–C coating, *Surf. Coat. Technol.*, 2018, vol. 335, pp. 327–333.
23. Wang, Y., Zhu, Sh., Gu, W., and Qi, X., Electric contact strengthening to improve the bonding between WC–Co coating and 45# steel substrate, *J. Therm. Spray Technol.*, 2010, vol. 19, no. 5, pp. 1142–1146.

24. Xu, M., Zhu, Sh., and Ding, H., Electrical contact strengthening of induction-clad Ni–40% WC composite coatings on 40Cr substrates, *Surf. Coat. Technol.*, 2015, vol. 279, pp. 32–38.

25. Yakovlev, S.A., Zamal'dinov, M.M., and Tatarov, L.G., Influence of electromechanical processing on structure and hardness of VT22 titanium alloy, *Uprochnyayushchie Tekhnol. Pokrytiya*, 2017, vol. 13, no. 10 (154), pp. 464–467.

26. Bagmutov, V.P., Vodop'yanov, V.I., Zakharov, I.N., and Denisevich, D.S., Relation between the fracture laws and the fatigue life of a surface-hardened pseudo-α titanium alloy, *Russ. Metall.* (Engl. Transl.), 2016, vol. 2016, no. 7, pp. 663–668.

27. Stachowiak, G.W. and Batchelor, A.W., Surface hardening and deposition of coatings on metals by a mobile source of localized electrical resistive heating, *J. Mater. Process. Technol.*, 1996, no. 57, pp. 288–297.

28. Kholopov, Yu.V., Zinchenko, A.G., and Savinykh, A.A., *Bezabrazivnaya ul'trazvukovaya finishnaya obrabotka metallov* (Non-Abrasive Ultrasonic Finishing Treatment of Metals), Leningrad: Leningrad. Dom Nauchno-Tekh. Propag., 1988.

29. Parshin, A.M. and Kirillov, N.V., Physical and structural aspects of alloys processing by concentrated energy sources, *Metally*, 1995, no. 3, pp. 122–127.

30. Bagmutov, V.P., Zakharov, I.N., and Denisevich, D.S., Solution of technological problems of inhomogeneous metallic bodies mechanics with the structure transformed under thermal force loading, *Vestn. Permsk. Nats. Issled. Politekh. Univ., Mekh.*, 2016, no. 1, pp. 5–25.

Translated by Bernard Gilbert